



# Visible light-controlled carbon monoxide delivery combined with the inhibitory activity of histone deacetylases from a manganese complex for an enhanced antitumor therapy

Hai-Lin Zhang<sup>a</sup>, Ya-Ting Yu<sup>a</sup>, Yi Wang<sup>a</sup>, Qi Tang<sup>a</sup>, Shi-Ping Yang<sup>b</sup>, Jin-Gang Liu<sup>a,\*</sup>

<sup>a</sup> Key Laboratory for Advanced Materials, School of Chemistry & Molecular Engineering, East China University of Science and Technology, Shanghai 200237, PR China

<sup>b</sup> Key Lab of Resource Chemistry of MOE & Shanghai Key Lab of Rare Earth Functional Materials, Shanghai Normal University, Shanghai 200234, PR China

## ARTICLE INFO

### Keywords:

Manganese carbonyl complexes  
Carbon monoxide  
Light-controlled release  
Histone deacetylase inhibitor  
Combined therapy

## ABSTRACT

Multifunctional drugs with synergistic effects have been widely developed to enhance the treatment efficiency of various diseases, such as malignant tumors. Herein, a novel bifunctional manganese(I)-based prodrug [MnBr(CO)<sub>3</sub>(AIPB)] (AIPB = N-(2-aminophen-yl)-4-(1H-imidazo[4,5-f][1,10]phenanthrolin-2-yl)benzamide) with inhibitory histone deacetylase (HDAC) activity and light-controlled carbon monoxide (CO) delivery was successfully designed and synthesized. [MnBr(CO)<sub>3</sub>(AIPB)] readily released CO under visible light irradiation ( $\lambda > 400$  nm) through which the amount of released CO could be controlled by manipulating light power density and illumination time. In the absence of light irradiation, the cytotoxic effect of [MnBr(CO)<sub>3</sub>(AIPB)] on cancer cells was greater than that of the commercially available HDAC inhibitor MS-275. Consequently, with a combination of CO delivery and HDAC inhibitory activity, [MnBr(CO)<sub>3</sub>(AIPB)] showed a remarkably enhanced antitumor effect on HeLa cells (IC<sub>50</sub> = 3.2  $\mu$ M) under visible light irradiation. Therefore, this approach shows potential for the development of medicinal metal complexes for combined antitumor therapies.

## 1. Introduction

Histone deacetylases (HDACs) promote the removal of the acetyl group from the lysine residue of the histone core and play significant roles in the dynamic balancing process of lysine deacetylation and acetylation [1,2]. However, an excessive HDAC activity causes the aberrant expression of various genes, leading to chromatin condensation and transcriptional repression associated with cancer cell proliferation, metabolic disorders, and apoptosis regulation [3,4]. Correspondingly, HDAC inhibitors (HDACIs) are potential antitumor agents that block abnormal HDAC deacetylation to restore gene transcription, thereby inhibiting cancer cell proliferation, angiogenesis, invasion, differentiation, and metastasis; promoting cell cycle arrest and apoptosis; and simultaneously enhancing host immune responses [5–7]. Therefore, various kinds of HDACIs, including benzamides (entinostat, MS-275) [8], cyclic tetrapeptide (romidepsin, FK-228) [9], hydroxamic acids

(vorinostat, SAHA) [10], and short-chain fatty acids [11], have been designed and synthesized for cancer treatment. Zn<sup>2+</sup>-dependent HDACs generally have a common pharmacophore, i.e., a zinc-binding group (ZBG), a hydrophobic capping group, and a linker to connect the ZBG and the capping group, among which the ZBG readily coordinates with the active site Zn<sup>2+</sup> to inhibit HDAC activity (Fig. 1A) [12]. This structure provides a basis for exploring new HDACIs as anticancer agents.

HDACs are mainly used to treat malignant tumors in the hematological system [13,14]. They have a relatively weaker effect on solid tumors than HDACs on hematological tumors. Therefore, the design and preparation of novel HDACIs with combined chemo/photodynamic therapy are effective strategies to enhance their anticancer activity. Marmion and co-workers [15] developed a Pt complex of *cis*-[Pt<sup>II</sup>(NH<sub>3</sub>)<sub>2</sub>(malSAHAH<sub>2</sub>)] that contains a SAHA inhibitor, and the complex exhibited DNA binding and HDAC inhibitory activity; thus, the treatment efficacy against tumors is enhanced. Mao and co-workers [16]

**Abbreviations:** HDAC, Histone deacetylase; HDACI, HDAC inhibitor; GSH, Glutathione; ZBG, Zinc-binding group; Hb, Hemoglobin; photoCORM, Photo-activated CO-releasing molecule; AIPB, N-(2-aminophen-yl)-4-(1H-imidazo[4,5-f][1,10]phenanthrolin-2-yl)benzamide; PDO, 10-Phenanthroline-5,6-dione; HNCP, 2-(4-carboxyphenyl)imidazo(4,5-f)(1,10) phenanthroline; HOBT, 1-hydroxybenzotriazole; DCC, N,N-dicyclohexylcarbodiimide; PIPB, 4-(1H-imidazo[4,5-f][1,10]phenanthrolin-2-yl)-N-phenylbenzamide; HbCO, Carboxyhemoglobin; PBS, Phosphate buffered saline; MTT, 3-(4,5-Dimethylthiazol-2-yl)-2,5-diphenyltetrazolium bromide.

\* Corresponding author.

E-mail address: [liujingang@ecust.edu.cn](mailto:liujingang@ecust.edu.cn) (J.-G. Liu).

<https://doi.org/10.1016/j.jinorgbio.2021.111354>

Received 18 August 2020; Received in revised form 24 December 2020; Accepted 3 January 2021

Available online 8 January 2021

0162-0134/© 2021 Elsevier Inc. All rights reserved.

explored a series of cyclometalated Ir(III) complexes composed of a hydroxamic acid inhibitor, which exhibits a synergistic inhibitory effect on HDAC activity and photodynamic therapy by producing reactive oxygen species under UV or visible light irradiation. In addition, HDACIs have been incorporated with therapeutic gas-releasing molecules for synergistic therapy. Zhang et al. reported a series of nitric oxide (NO)-releasing molecules whose NO donor is connected to a HDACI via various linkers. The released NO combined with the inhibitory effect of HDACI can induce apoptosis and G1 phase arrest in HEL cells [17]. However, the uncontrollable delivery of NO molecules greatly limits the practical application of gas therapy.

As an emerging therapeutic gas molecule, carbon monoxide (CO) has been applied to treat various diseases, including cancer [18,19]. Endogenous CO, a signaling molecule, plays significant roles in the physiological activities of nerve transmission, cardiovascular regulation, inflammation, apoptosis, and immune responses [20,21]. Notably, an excessive amount of CO detracts the oxygen-binding capacity of hemoglobin (Hb), resulting in serious cytotoxicity [22–24]. Therefore, a high CO concentration is critical to show a desirable therapeutic efficacy against cancer cells. However, the inherent toxicity of CO significantly limits its direct application in cancer therapy. Consequently, stimulus-responsive CO donor molecules for the controlled on-demand delivery of CO have been developed; in this process, the release of CO is triggered by different stimuli, such as pH [25,26], Glutathione (GSH) [27], H<sub>2</sub>O<sub>2</sub> [28,29], enzymes [30], magnetic heating [31,32], and light [33–35]. Various photo-activated CO-releasing molecules (photoCORMs) have been widely explored because of their non-invasiveness, light maneuverability, and precise controllability of CO delivery [36–40], among which the Mn(I)-based photoCORMs have been mostly studied due to the feasibility to release CO under visible light with relative low-power density. This can alleviate light-induced damage to healthy tissues and cells [38]. In addition, as one of the essential trace elements for human body, the Mn element can be effectively regulated by metabolism [41]. However, photoCORMs incorporated with HDACI for combined therapies are lacking.

Herein, we prepared a novel manganese complex [MnBr(CO)<sub>3</sub>(A-PIPB)] (A-PIPB = N-(2-aminophen-yl)-4-(1H-imidazo[4,5-f][1,10]phenanthrolin-2-yl)benzamide) as a bifunctional photoCORM for HDAC activity inhibition and visible light-controlled CO delivery (Fig. 1B). [MnBr(CO)<sub>3</sub>(A-PIPB)] contains a mimic of the classic benzamide HDAC inhibitor MS-275, whose phenanthroline derivative serves as the capping group of HDACI, benzamide functions as the ZBG, and benzene participates as a linker to connect the ZBG and the capping group (Fig. 1A). The results showed that the HDAC inhibition efficiency of [MnBr(CO)<sub>3</sub>(A-PIPB)] is higher than that of MS-275 in the dark, and CO was instantly released upon visible light irradiation. Consequently, the anticancer efficacy against cancerous HeLa cells was remarkably enhanced.

## 2. Materials and methods

### 2.1. Materials

All the reagents were used as purchased commercially without further purification unless otherwise noted. 10-Phenanthroline-5,6-dione (PDO) [42] and 2-(4-carboxyphenyl)imidazo(4,5-f)(1,10) phenanthroline (HNCP) [43] were synthesized in accordance with previously reported methods.

Human cervical carcinoma cells (HeLa cells) were obtained from the Shanghai Institute for Biological Sciences, the Chinese Academy of Sciences (CAS, China).

### 2.2. Physical measurement

UV–vis absorption spectra, Fourier transform infrared (FT-IR) spectra, ESI–MS spectra, fluorescence spectra, and <sup>1</sup>H NMR spectra were acquired in accordance with our previously described methods [44,45].

### 2.3. Synthesis of A-PIPB

A cooled mixture of conc. H<sub>2</sub>SO<sub>4</sub>–HNO<sub>3</sub> (60 mL, 2:1, v/v) was added with 1,10-phenanthroline (4 g, 22 mmol) and KBr (4 g, 33 mmol) and stirred at 130 °C for 3 h. A yellow solution was cautiously neutralized with NaOH solution (10 mol·L<sup>-1</sup>) until its pH was neutral. The resulting mixture was extracted with CH<sub>2</sub>Cl<sub>2</sub> and dried with anhydrous Na<sub>2</sub>SO<sub>4</sub>. Afterward, solvents were removed, and PDO was obtained as a yellow solid. Then, PDO (0.420 g, 2 mmol), 4-carboxybenzaldehyde (0.360 g, 2.4 mmol), and CH<sub>3</sub>COONH<sub>4</sub> (3.2 g, 41.5 mmol) were mixed in 50 mL of CH<sub>3</sub>COOH and stirred at 130 °C for 4 h. After being cooled to room temperature, the solution was adjusted to pH 5.0 by adding NH<sub>3</sub>·H<sub>2</sub>O (25 wt%) solution while stirring, and HNCP was dried in vacuum. HNCP (0.34 g, 0.79 mmol), 1,2-diaminobenzene (0.325 g, 3 mmol), 1-hydroxybenzotriazole (HOBT; 0.135 g, 1 mmol), N,N-dicyclohexylcarbodiimide (DCC; 0.248 g, 1.2 mmol), and triethylamine (167 μL) were dissolved in 30 mL of DMF at 4 °C for 2 h while stirring. The resulting mixture was stirred at room temperature for 24 h under a N<sub>2</sub> atmosphere. The faint yellow solid was filtered, washed with CH<sub>2</sub>Cl<sub>2</sub> and Et<sub>2</sub>OH, and dried in vacuum. The reaction yielded 0.370 g (yield: 71.3%) of A-PIPB with the following properties: <sup>1</sup>H NMR (400 MHz, DMSO-*d*<sub>6</sub>): δ 13.95 (s, 1H), 9.84 (s, 1H), 9.07 (s, 2H), 8.99–8.97 (d, 2H), 8.44–8.42 (d, 2H), 8.25–8.23 (d, 2H), 7.92–7.84 (ddd, 2H), 7.21–7.19 (d, 2H), 7.02–6.98 (t, 1H), 6.82–6.80 (d, 1H), 6.64–6.61 (t, 1H), 5.05 (br, 1H) ppm. ESI–MS: *m/z*, [M + H]<sup>+</sup>: calcd. 431.2, found 431.2.

PIPB (PIPB = 4-(1H-imidazo[4,5-f][1,10]phenanthrolin-2-yl)-N-phenylbenzamide) as a control ligand, which lacks the amino group on the benzamide motif, was synthesized with a procedure similar to A-PIPB synthesis, but *o*-phenylenediamine was replaced with aniline. <sup>1</sup>H NMR

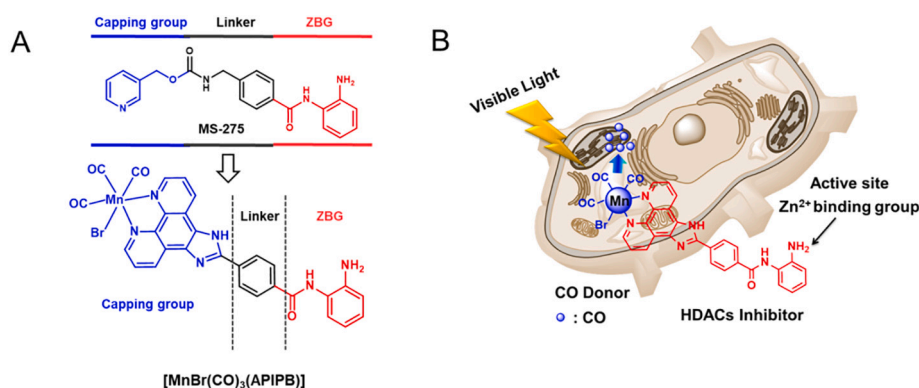


Fig. 1. (A) Design strategy of [MnBr(CO)<sub>3</sub>(A-PIPB)]. (B) Schematic of [MnBr(CO)<sub>3</sub>(A-PIPB)].

(400 MHz, DMSO- $d_6$ ):  $\delta$  13.96 (s, 1H), 10.41(s, 1H), 9.06(s, 2H), 8.98–8.96 (d, 2H), 8.45–8.43 (d, 2H), 8.22–8.20 (d, 2H), 7.91–7.84 (ddd, 2H), 7.83–7.81 (d, 2H), 7.41–7.37 (t, 2H), 7.15–7.12 (t, 1H) ppm. ESI-MS:  $m/z$  [M + H]<sup>+</sup>: calcd. 416.2, found 416.2.

#### 2.4. Synthesis of [MnBr(CO)<sub>3</sub>(APIPB)]

In this procedure, 0.302 g of 1.1 mmol Mn(CO)<sub>5</sub>Br and 0.430 g of mmol APIPB were added to 20 mL of CH<sub>2</sub>Cl<sub>2</sub> and heated at reflux for 5 h under a N<sub>2</sub> atmosphere. The solution was cooled to room temperature and stored at 4 °C overnight. The obtained yellow solid was filtered, washed with cold CH<sub>2</sub>Cl<sub>2</sub>, and collected by freeze-drying. The reaction yielded 0.590 g (yield: 90.6%) of [MnBr(CO)<sub>3</sub>(APIPB)]. <sup>1</sup>H NMR (400 MHz, DMSO- $d_6$ ):  $\delta$  14.38 (s, 1H), 9.86 (s, 1H), 9.55–9.54 (d, 2H), 9.19–9.17 (d, 2H), 8.44–8.42 (d, 2H), 8.27–8.26 (d, 2H), 8.17–8.13 (m, 2H), 7.23–7.21 (d, 1H), 7.03–6.99 (t, 1H), 6.83–6.81 (d, 1H), 6.65–6.62 (t, 1H), 4.99 (s, 2H) ppm. ESI-MS:  $m/z$  [M-3CO-Br]<sup>+</sup>: calcd. 485.1, found 485.1. Anal. Calcd. for C<sub>29</sub>H<sub>18</sub>N<sub>6</sub>O<sub>4</sub>BrMn (%): C, 53.64; H, 2.79; N, 12.94. Found: C, 53.71; H, 2.78; N, 12.97.

In the synthesis of the control complex [MnBr(CO)<sub>3</sub>(PIPB)], PIPB was used instead of APIPB, and the remaining experimental steps were the same as above. <sup>1</sup>H NMR (400 MHz, DMSO- $d_6$ ):  $\delta$  14.39 (s, 1H), 10.42 (s, 1H), 9.55–9.54 (d, 2H), 9.18–9.17 (d, 2H), 8.45–8.44 (d, 2H), 8.25–8.23 (d, 2H), 8.15 (brs, 2H), 7.83–7.82 (d, 2H), 7.41–7.38 (t, 2H), 7.15–7.12 (t, 1H) ppm. ESI-MS:  $m/z$  [M-3CO-Br]<sup>+</sup>: calcd. 470.1, found 470.1. Anal. Calcd. for C<sub>29</sub>H<sub>17</sub>N<sub>5</sub>O<sub>4</sub>BrMn (%): C, 54.91; H, 2.70; N, 11.04. Found: C, 54.99; H, 2.69; N, 11.07.

#### 2.5. Light-triggered CO release

##### 2.5.1. Measurement of CO release via the hemoglobin method

CO release was detected by spectrophotometrically measuring the conversion of Hb to carboxyhemoglobin (HbCO) [46]. In brief, 4.2  $\mu$ M Hb was dissolved completely in 10 mM phosphate buffered saline (PBS; pH = 7.4) and reduced by adding 1.6 mg of 9.2 mmol sodium dithionite (SDT) in a N<sub>2</sub> atmosphere. Next, [MnBr(CO)<sub>3</sub>(APIPB)] was suspended in D. I. water, deoxygenated with N<sub>2</sub>, and added to the above Hb solution. Then, the 4 mL solution was sealed immediately in a quartz cuvette, and the mixture was irradiated with different intensities of visible light ( $\lambda$  > 400 nm). CO release was monitored by detecting the spectral changes (350–600 nm) in HbCO in the PBS solution at different intervals with a UV-vis spectrophotometer. The UV adsorption spectral changes of the solution at 420 nm were taken to calculate the concentration of the released CO in accordance with Beer-Lambert's law expressed in Eq. (1):

$$X\% = \frac{E_x - E_0'}{E_{100} - E_0} \times 100\% \quad (1)$$

where X% is the cumulative release percentage of CO, E<sub>100</sub> is the absorbance value when Hb is converted completely to HbCO, E<sub>0</sub> is the initial absorbance value, and E<sub>x</sub> and E<sub>0</sub>' are the absorbance values after light exposure and without light exposure, respectively.

##### 2.5.2. Measurement of CO release by using a fluorescent probe

In addition to the Hb method, a fluorescent CO probe (FL-CO-1 + PbCl<sub>2</sub>) was employed to measure the CO release. FL-CO-1 was synthesized in accordance with a previously reported method [47]. The product of FL-CO-1 with CO generated a green fluorescence (excitation: 490 nm, emission: 516 nm). The probe system (5  $\mu$ M probe + 5  $\mu$ M PdCl<sub>2</sub>) was mixed with the [MnBr(CO)<sub>3</sub>(APIPB)] solution and sealed in a quartz cuvette. Then, the mixture was irradiated with visible light, and the fluorescence spectra were obtained using a fluorescence spectrophotometer in real time. The released CO was detected by determining the fluorescence intensities at 516 nm.

#### 2.6. MTT assay

##### 2.6.1. Cytotoxicity test in the dark

HeLa cells were plated in a 96-well plate at a density of  $5 \times 10^4$  cells per well and incubated at 37 °C in 5% CO<sub>2</sub> for 24 h. Then, they were incubated with different concentrations (0, 2, 5, 10, and 25  $\mu$ M) of [MnBr(CO)<sub>3</sub>(APIPB)], [MnBr(CO)<sub>3</sub>(PIPB)], APIPB, and MS-275 for 16 h. And the solution in each well was then aspirated and rinsed with PBS. The background value was then measured with a microplate reader. An MTT solution (100  $\mu$ L, 0.5 mg/mL) was added to each well. After incubation for 3–4 h, the MTT residue in each well was aspirated, and 150  $\mu$ L of DMSO was added to lyse the formazan crystals. Cell viability was detected on the basis of the absorbance at 490 nm by using a multi-functional microplate reader.

##### 2.6.2. Cytotoxicity test under visible light irradiation

The process of cell plating in this procedure was the same as the steps described in Section 2.6.1. After the cells were incubated with different concentrations (0, 2, 5, 10, and 25  $\mu$ M) of [MnBr(CO)<sub>3</sub>(APIPB)], [MnBr(CO)<sub>3</sub>(PIPB)], APIPB, and MS-275 for 12 h, visible light was applied ( $\lambda$  > 400 nm, 200 mW/cm<sup>2</sup>, 10 min), and the cells were incubated for 4 h. The same procedures as above were performed to obtain the final absorbance at 490 nm by using a microplate reader.

### 3. Results and discussion

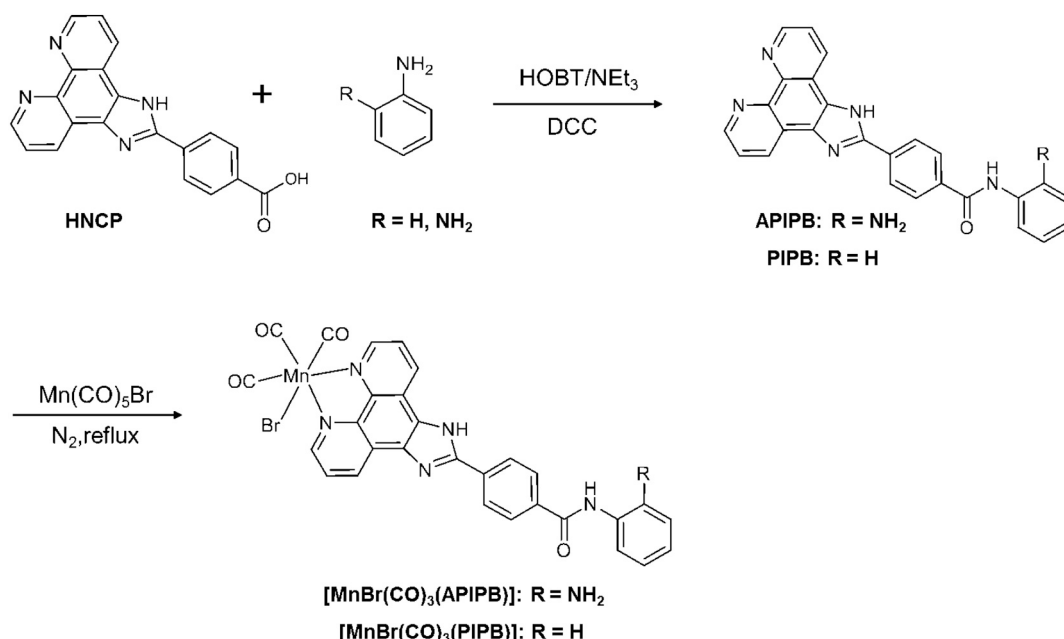
#### 3.1. Synthesis and characterization of [MnBr(CO)<sub>3</sub>(APIPB)]

Manganese carbonyl complexes were synthesized in accordance with the procedure illustrated in Scheme 1. Firstly, HNCP was obtained with previously reported methods [42,43]. Then, it reacted with *o*-phenylenediamine in the presence of HOBT and DCC, yielding the phenanthroline derivative APIPB. The final complex [MnBr(CO)<sub>3</sub>(APIPB)] was synthesized through the coordination of the APIPB ligand with Mn(CO)<sub>5</sub>Br in a dichloromethane solution. The <sup>1</sup>H NMR spectra of [MnBr(CO)<sub>3</sub>(APIPB)] revealed that the protons of phenanthroline in APIPB experienced a downfield chemical shift when APIPB coordinated with Mn(CO)<sub>5</sub>Br, whereas the chemical shift of other protons in APIPB was almost unchanged (Figs. S1). This result indicated that APIPB successfully coordinated with the manganese center. Besides, the FT-IR spectra of [MnBr(CO)<sub>3</sub>(APIPB)] showed strong peaks at 2030 and 1931 cm<sup>-1</sup> that could be assigned to the  $\nu$ (CO) of the carbonyl group (Fig. 2A). These bands shifted to a lower wavenumber relative to the precursor compound MnBr(CO)<sub>5</sub> (2054 and 1995 cm<sup>-1</sup>). Furthermore, the UV-vis spectra of [MnBr(CO)<sub>3</sub>(APIPB)] exhibited prominent absorption peaks at 280 and 331 nm that extended to the visible region (Fig. 2B), where the peaks in the UV region corresponded to the characteristic absorption peaks of APIPB. The visible absorption of [MnBr(CO)<sub>3</sub>(APIPB)] indicated that the complex likely favored the visible light-triggered CO release.

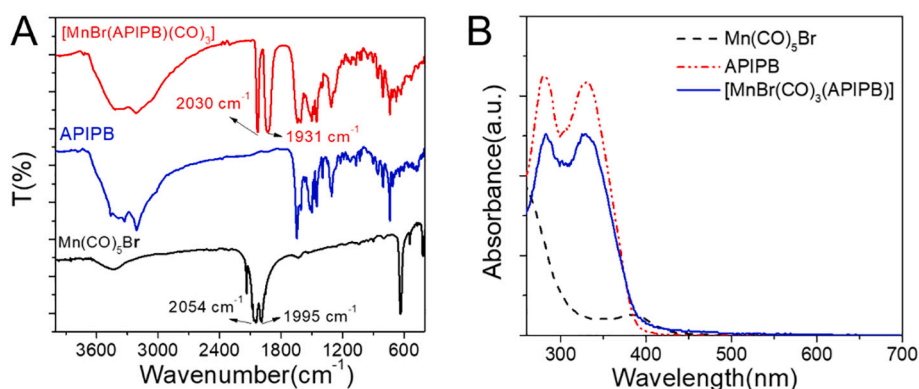
#### 3.2. Visible light-controlled CO release

CO readily reacts with Hb to form HbCO, which shows characteristic absorption changes with the Soret band (410–425 nm) and the Q-bands (540–570 nm) in the visible region; the Soret band is very sensitive to the degree of Hb carboxylation [48]. Therefore, visible light-triggered CO release from [MnBr(CO)<sub>3</sub>(APIPB)] was measured with the Hb method in accordance with Beer-Lambert's law (Scheme S1). When the solution of [MnBr(CO)<sub>3</sub>(APIPB)] was irradiated with visible light ( $\lambda$  > 400 nm), the UV-vis spectra of the reduced Hb experienced distinct spectral changes; that is, the Soret band shifted from 430 to 420 nm, and the Q-bands were developed at 540 and 570 nm, showing the characteristic absorption peaks of HbCO (Fig. 3A).

The amount of CO released was investigated under the irradiation of visible light with different power densities and complex concentrations.



Scheme 1. Synthesis route of manganese carbonyl complexes.

Fig. 2. FT-IR (A) and UV-vis spectra (B) of  $[\text{MnBr(CO)}_3(\text{AIPiPB})]$ , AIPiPB, and  $\text{Mn(CO)}_5\text{Br}$ .

The CO release rate reduced as exposure time under visible light irradiation at a certain power density was prolonged. Conversely, this rate increased as the light power density was enhanced. The visible light irradiation ( $\lambda > 400$  nm,  $400 \text{ mW/cm}^2$ ) of the  $[\text{MnBr(CO)}_3(\text{AIPiPB})]$  solution resulted in an immediate CO release that produced about 90% of CO from the complex within 2 min (Fig. 3B). The amount of released CO was positively proportional to the applied light intensity (Fig. 3B) and the complex concentration (Fig. 3C). Under a dark condition, CO was not released, suggesting the good stability of  $[\text{MnBr(CO)}_3(\text{AIPiPB})]$  in the PBS solution in the absence of light irradiation. When visible light was turned on, the CO was released immediately; once visible light was turned off, the release of CO instantly stopped (Fig. 3D). As a result, the repetitive on-off switching of visible light could readily control the release of CO from the complex. Therefore, the release of CO from  $[\text{MnBr(CO)}_3(\text{AIPiPB})]$  was completely controlled by light, and the CO concentration could be well controlled by manipulating the exposure time of applied light, light intensity, and complex concentration. To note that the complex  $[\text{MnBr(CO)}_3(\text{AIPiPB})]$  showed good stability after it was stored in PBS solution under dark condition for 7 days (Fig. S5A), and still maintained excellent CO release performance under visible light ( $\lambda > 400$  nm,  $200 \text{ mW/cm}^2$ ) irradiation (Fig. S5B). This kind of CO release property could be useful for clinical practices requiring the precise control of the on-demand dosage of CO for therapy. This property was

also significant for prolonging the drug efficacy and reducing the risk of CO poisoning.

The visible light-triggered release of CO from  $[\text{MnBr(CO)}_3(\text{AIPiPB})]$  was further verified with a CO fluorescence probe (FL-CO-1 +  $\text{PbCl}_2$ ) [47] and FT-IR spectra. The fluorescence intensity of the probe in the PBS solution increased significantly as the exposure time of  $[\text{MnBr(CO)}_3(\text{AIPiPB})]$  under visible light irradiation was prolonged (Fig. 4A). This result suggested that CO was released from the complex. The observed optical changes were attributed to the reduction of  $\text{Pd}^{2+}$  to  $\text{Pd}^0$  by CO, which mediated the Tsuji-Trost reaction of FL-CO-1 to produce fluorescein (or 2,7-dichlorofluorescein) with strong yellow-green fluorescence (Scheme S2). Because this process involves two steps, the response time to detect CO is somewhat extended. Furthermore, the FT-IR spectra of  $[\text{MnBr(CO)}_3(\text{AIPiPB})]$  revealed that the characteristic absorption peaks of CO at  $2030$  and  $1931 \text{ cm}^{-1}$  gradually diminished upon visible light irradiation (Fig. 4B), indicating the escape of CO from  $[\text{MnBr(CO)}_3(\text{AIPiPB})]$ .

### 3.3. Assessment of *in vitro* cytotoxicity

The cytotoxic effects of  $[\text{MnBr(CO)}_3(\text{AIPiPB})]$  were investigated using HeLa cells as a model cell line. MS-257 is a benzamide derivative and commercially available HDAC inhibitor used to treat hematological

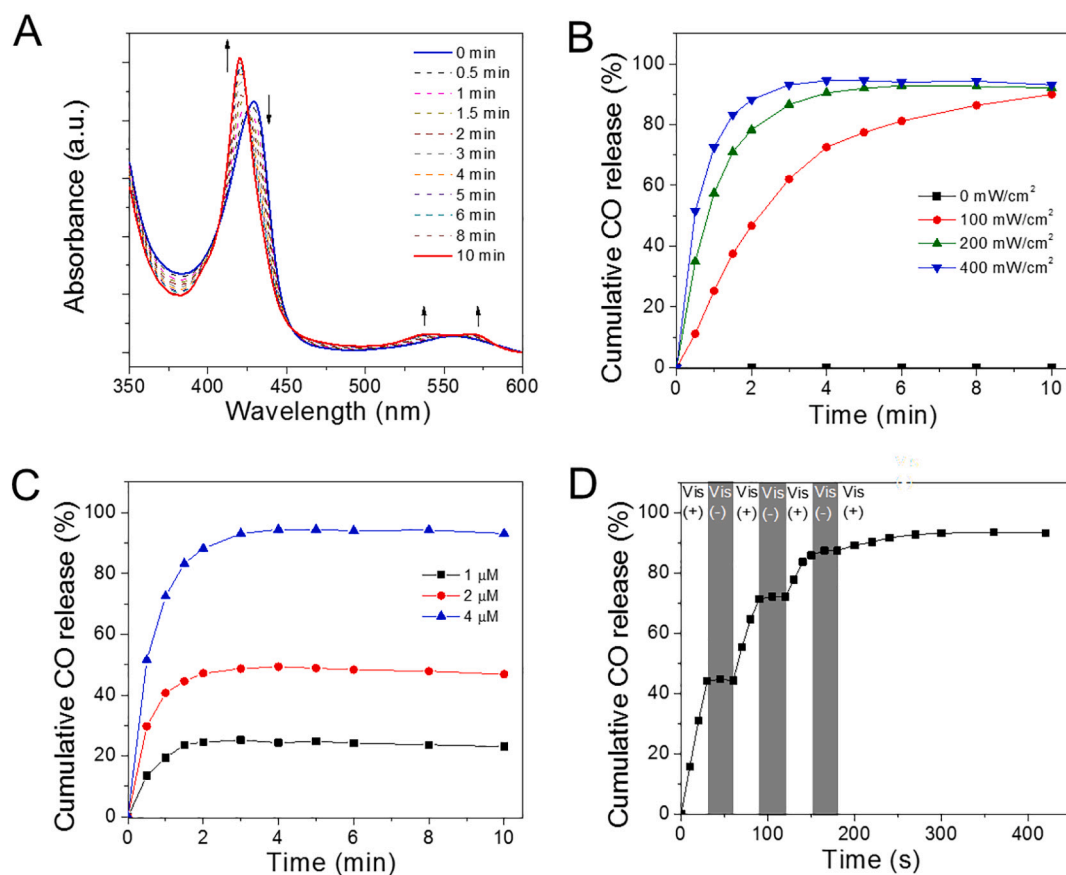


**Fig. 3.** Changes in the UV-Vis spectra of HbCO, indicating the release of CO from  $[\text{MnBr}(\text{CO})_3(\text{APIPB})]$  in a PBS solution under visible light irradiation (A). Release of CO under visible light irradiation with different light intensities (B) and  $[\text{MnBr}(\text{CO})_3(\text{APIPB})]$  concentrations (C). Visible light controllability of  $[\text{MnBr}(\text{CO})_3(\text{APIPB})]$  for CO release by switching the visible light on/off (D).

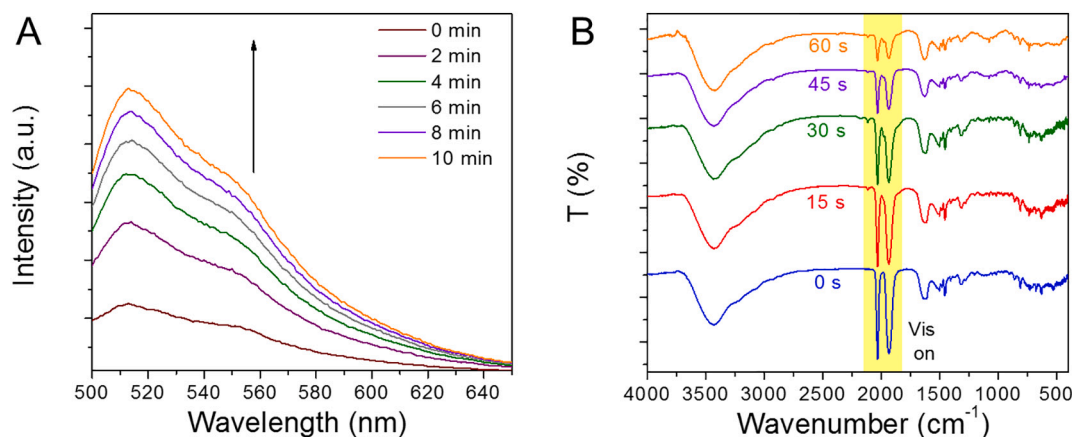


**Fig. 4.** (A) Fluorescence spectral changes in the CO probe system (FL-CO-1 +  $\text{PdCl}_2$ ) with the addition of  $[\text{MnBr}(\text{CO})_3(\text{APIPB})]$  in the PBS solution under visible light irradiation. (B) FT-IR spectral changes in  $[\text{MnBr}(\text{CO})_3(\text{APIPB})]$  solid sample under visible light irradiation.

malignancies and solid tumors. In this study, different concentrations of the complex and MS-275 were incubated with HeLa cells at concentrations varying from 0  $\mu\text{M}$  to 25  $\mu\text{M}$  in the absence of light irradiation to evaluate the enzyme inhibitory effect of  $[\text{MnBr}(\text{CO})_3(\text{APIPB})]$ . In Fig. 5A, the cytotoxic effect of the APIPB ligand was similar to that of MS-275, and the viability of the  $[\text{MnBr}(\text{CO})_3(\text{APIPB})]$  (25  $\mu\text{M}$ )-treated cells (53%) was lower than that of the MS-275-treated ones (68%) after incubation under a dark condition. To note that significantly higher viability of the  $[\text{MnBr}(\text{CO})_3(\text{APIPB})]$ -treated normal LO2 cells was observed under the similar experimental conditions (Fig. S7B). These

results clearly suggested that  $[\text{MnBr}(\text{CO})_3(\text{APIPB})]$  elicited an excellent HDAC inhibitory effect on cancerous cells even without releasing CO.

MTT cytotoxicity analysis was then performed using  $[\text{MnBr}(\text{CO})_3(\text{APIPB})]$ -treated HeLa cells in the presence of visible light illumination.  $[\text{MnBr}(\text{CO})_3(\text{PIPB})]$  that lacked the *ortho* amino group on the benzamide structure was taken as the control sample of  $[\text{MnBr}(\text{CO})_3(\text{APIPB})]$ . This amino group functioned as a crucial reaction site of ZBGs and determined the inhibitory activity of benzamide in HDACIs. After the  $[\text{MnBr}(\text{CO})_3(\text{APIPB})]$  (25  $\mu\text{M}$ )-treated HeLa cells were irradiated with visible light ( $\lambda > 400 \text{ nm}$ , 200  $\text{mW}/\text{cm}^2$ ) for 10 min, numerous

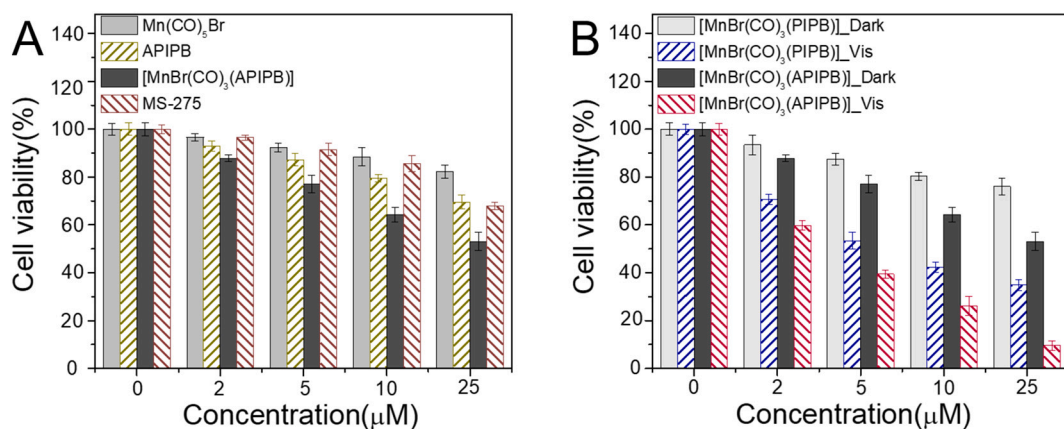


**Fig. 5.** (A) MTT cytotoxicity assays of HeLa cells treated with Mn(CO)<sub>5</sub>Br, APIPb, [MnBr(CO)<sub>3</sub>(APIPB)], and MS-275 at different concentrations under the dark condition. (B) MTT cytotoxicity assays of HeLa cells treated with [MnBr(CO)<sub>3</sub>(PIPB)] and [MnBr(CO)<sub>3</sub>(APIPB)] at different concentrations under the dark and visible light irradiation conditions.

HeLa cells were killed, and their viability was less than 9% (Fig. 5B). Conversely, the viability of the [MnBr(CO)<sub>3</sub>(PIPB)]-treated cells (35%) was relatively higher under the same experimental conditions. The cytotoxicity difference between [MnBr(CO)<sub>3</sub>(APIPB)] and [MnBr(CO)<sub>3</sub>(PIPB)] was likely attributed to the absence of the *ortho* amino group in the PIPB ligand, which rendered [MnBr(CO)<sub>3</sub>(PIPB)] with a neglected inhibitory effect on HDACs. IC<sub>50</sub> of [MnBr(CO)<sub>3</sub>(APIPB)] toward HeLa cells under light irradiation was approximately 3.2 μM, which is less than the half of IC<sub>50</sub> of [MnBr(CO)<sub>3</sub>(PIPB)]. Consequently, the anticancer effect of [MnBr(CO)<sub>3</sub>(APIPB)] was improved by combining the pharmaceutical efficacy of CO and the enzyme inhibitory activity of HDACs. Therefore, the synthesized complex could be a promising anticancer agent.

#### 4. Conclusion

In this study, a novel bifunctional manganese carbonyl complex ([MnBr(CO)<sub>3</sub>(APIPB)]) that contains an HDAC inhibitor mimic was designed and successfully synthesized. This complex exhibited a high HDAC inhibition efficiency and visible light-triggered CO release, whose amount was readily controlled by tuning the applied light power density, illumination time, and complex concentration. The release of CO from [MnBr(CO)<sub>3</sub>(APIPB)] was spectroscopically confirmed via its reaction with hemoglobin, CO fluorescence probe (FL-CO-1 + PbCl<sub>2</sub>), and FT-IR spectroscopy. CO was instantly liberated and more than 90% of CO was released from [MnBr(CO)<sub>3</sub>(APIPB)] within minutes under visible light irradiation (λ > 400 nm, 400 mW/cm<sup>2</sup>). The cytotoxic and anticancer effects of [MnBr(CO)<sub>3</sub>(APIPB)] against cancerous HeLa cells in the dark were greater than those of MS-275. Under visible light irradiation, cell mortality was remarkably enhanced with IC<sub>50</sub> of as low as 3.2 μM, which was attributed to the synergistic effect of the released CO and the inhibitory effect of HDAC. Consequently, with a combination of the CO release and the HDAC inhibitory activity, [MnBr(CO)<sub>3</sub>(APIPB)] showed an impressively enhanced antitumor effect on HeLa cells under visible light irradiation. Thus, [MnBr(CO)<sub>3</sub>(APIPB)] served as a novel example of an application that combined gas therapy with enzyme inhibition for an efficacious tumor treatment.

#### Author statement

This manuscript or its contents in other forms has not been published previously and/or is not under consideration for publication elsewhere at the time of submission. And all the authors approved to publish this work in *Journal of Inorganic Biochemistry*.

#### Declaration of Competing Interest

The authors have no competing interests to declare.

#### Acknowledgement

This study was financially supported by the NSF of China (No. 21571062), the Program for Professor of Special Appointment (Eastern Scholar) at Shanghai Institutions of Higher Learning.

#### Appendix A. Supplementary data

Supplementary data to this article can be found online at <https://doi.org/10.1016/j.jinorgbio.2021.111354>.

#### References

- [1] L. Galluzzi, L. Senovilla, I. Vitale, J. Michels, I. Martins, O. Kepp, M. Castedo, G. Kroemer, *Oncogene* 31 (2012) 1869–1883.
- [2] C.H. Leung, H.J. Zhong, D.S.H. Chan, D.L. Ma, *Coord. Chem. Rev.* 257 (2013) 1764–1776.
- [3] M. Paris, M. Porcelloni, M. Binascchi, D. Fattori, *J. Med. Chem.* 51 (2008) 1505–1529.
- [4] P. Bertrand, *Eur. J. Med. Chem.* 45 (2010) 2095–2116.
- [5] S.A.M. Thiagalingam, K.H. Cheng, H.J. Lee, N. Mineva, *Ann. N. Y. Acad. Sci.* 983 (2003) 84–100.
- [6] P.A. Marks, V.M. Richon, R.A. Rifkind, *J. Natl. Cancer Inst.* 92 (2000) 1210–1216.
- [7] C.B. Yoo, P.A. Jones, *Nat. Rev. Drug Discov.* 5 (2006) 37–50.
- [8] T. Suzuki, T. Ando, K. Tsuchiya, N. Fukazawa, A. Saito, Y. Mariko, T. Yamashita, O. Nakanishi, *J. Med. Chem.* 42 (1999) 3001–3003.
- [9] R. Furumai, A. Matsuyama, N. Kobashi, K.H. Lee, M. Nishiyama, H. Nakajima, A. Tanaka, Y. Komatsu, N. Nishino, M. Yoshida, S. Horinouchi, *Cancer Res.* 62 (2002) 4916–4921.
- [10] S. Grant, C. Easley, P. Kirkpatrick, *Nat. Rev. Drug Discov.* 6 (2007) 21–22.
- [11] N. Khan, M. Jeffers, S. Kumar, C. Hackett, F. Boldog, N. Khramtsov, X. Qian, E. Mills, S.C. Berghs, N. Carey, P.W. Finn, L.S. Collins, A. Tumber, J.W. Ritchie, P. B. Jensen, H.S. Lichtenstein, M. Sehested, *Biochem. J.* 409 (2008) 581–589.
- [12] C. Seidel, M. Schnekenburger, C. Zwergel, F. Gaascht, A. Mai, M. Dicato, G. Kirsch, S. Valente, M. Diederich, *Bioorg. Med. Chem. Lett.* 24 (2014) 3797–3801.
- [13] R. Benedetti, M. Conte, L. Altucci, *Antioxid. Redox Signal.* 23 (2015) 99–126.
- [14] L. Verna, J. Whysner, G.M. Williams, *Clin. Pharmacol. Ther.* 71 (1996) 83–105.
- [15] D. Griffith, M.P. Morgan, C.J. Marmion, *Chem. Commun.* 44 (2009) 6735–6737.
- [16] R.R. Ye, C.P. Tan, L. He, M.H. Chen, L.N. Ji, Z.W. Mao, *Chem. Commun.* 50 (2014) 10945–10948.
- [17] W.W. Duan, J. Li, E.S. Inks, J.C. Chou, Y.P. Jia, X.J. Chu, X.Y. Li, W.F. Xu, Y. J. Zhang, *J. Med. Chem.* 58 (2015) 4325–4338.
- [18] H.L. Yan, J.F. Du, S. Zhu, G.J. Nie, H. Zhang, Z.J. Gu, Y.L. Zhao, *Small* 15 (2019) 1904382.
- [19] Y. Zhou, W.Q. Yu, J. Cao, H.L. Gao, *Biomaterials* 255 (2020) 120193.
- [20] R. Motterlini, L.E. Otterbein, *Nat. Rev. Drug Discov.* 9 (2010) 728–743.
- [21] X.X. Yao, P. Yang, Z.K. Jin, Q. Jiang, R.R. Guo, R.H. Xie, Q.J. He, W.L. Yang, *Biomaterials* 197 (2019) 268–283.
- [22] B. Wegiel, D. Gallo, E. Csizmadia, C. Harris, J. Belcher, G.M. Vercellotti, N. Penacho, P. Seth, V. Sukhatme, A. Ahmed, P.P. Pandolfi, L. Helczynski, A. Bjartell, J.L. Persson, L.E. Otterbein, *Cancer Res.* 73 (2013) 7009–7021.

- [23] R. Foresti, M.G. Bani-Hani, R. Motterlini, *Intensive Care Med.* 34 (2008) 649–658.
- [24] G. Dördelmann, H. Pfeiffer, A. Birkner, U. Schatzschneider, *Inorg. Chem.* 50 (2011) 4362–4367.
- [25] F. Zobi, A. Degonda, M.C. Schaub, A.Y. Bogdanova, *Inorg. Chem.* 49 (2010) 7313–7322.
- [26] X. Ji, Z. Pan, C. Li, T. Kang, L.K.C. De La Cruz, L. Yang, Z. Yuan, B. Ke, B. Wang, *J. Med. Chem.* 62 (2019) 3163–3168.
- [27] C.J. Gao, X.H. Liang, Z.X. Guo, B.P. Jiang, X.M. Liu, X.C. Shen, *ACS Omega* 3 (2018) 2683–2689.
- [28] S. Fayad-Kobeissi, J. Ratovonantenaina, H. Dabiré, J.L. Wilson, A.M. Rodriguez, A. Berdeux, J. Dubois-Randé, B.E. Mann, R. Motterlini, R. Foresti, *Biochem. Pharmacol.* 102 (2015) 64–77.
- [29] Z. Jin, Y. Wen, L. Xiong, T. Yang, P. Zhao, L. Tan, T. Wang, Z. Qian, B.L. Su, Q. J. He, *Chem. Commun.* 53 (2017) 5557–5560.
- [30] N.S. Sitnikov, Y. Li, D. Zhang, B. Yard, H. Schmalz, *Angew. Chem. Int. Ed.* 54 (2015) 12314–12318.
- [31] P.C. Kunz, H. Meyer, J. Barthel, S. Sollazzo, A.M. Schmidt, C. Janiak, *Chem. Commun.* 49 (2013) 4896–4898.
- [32] H. Meyer, F. Winkler, P. Kunz, A.M. Schmidt, A. Hamacher, M.U. Kassack, C. Janiak, *Inorg. Chem.* 54 (2015) 11236–11246.
- [33] E. Palao, T. Slanina, L. Muchová, T. Šolomek, L. Vitek, P. Klán, *J. Am. Chem. Soc.* 138 (2016) 126–133.
- [34] T. Soboleva, H.J. Esquer, A.D. Benninghoff, L.M. Berreau, *J. Am. Chem. Soc.* 139 (2017) 9435–9438.
- [35] S.H.C. Askes, G.U. Reddy, R. Wyrwa, S. Bonnet, A. Schiller, *J. Am. Chem. Soc.* 139 (2017) 15292–15295.
- [36] S. Pordel, J.K. White, *Inorg. Chim. Acta* 500 (2020) 119206.
- [37] P.C. Ford, *Coord. Chem. Rev.* 376 (2018) 548–564.
- [38] M.N. Pinto, P.K. Mascharak, *J. Photochem. Photobiol. C* 42 (2020) 100341.
- [39] M. Faizan, N. Muhammad, K.U.K. Niazi, Y.X. Hu, Y.Y. Wang, Y. Wu, H.M. Sun, R. X. Liu, W.S. Dong, W.Q. Zhang, Z.W. Gao, *Materials* 12 (2019) 1643.
- [40] T. Slanina, P. Šebej, *Photochem. Photobiol. Sci.* 17 (2018) 692–710.
- [41] Z. Liu, S.J. Zhang, H. Liu, M.L. Zhao, H.L. Yao, L.L. Zhang, W.J. Peng, Y. Chen, *Biomaterials* 155 (2018) 54–63.
- [42] P.Y. Ma, F.H. Liang, D. Wang, Q.Q. Yang, Z.Q. Yang, D.J. Gao, Y. Yu, D.Q. Song, X. H. Wang, *Dyes Pigments* 122 (2015) 224–230.
- [43] Y.Q. Wei, Y.F. Yu, K.C. Wu, *Cryst. Growth Des.* 7 (2007) 2262–2264.
- [44] Y.H. Li, M. Guo, S.W. Shi, Q.L. Zhang, S.P. Yang, J.G. Liu, *J. Mater. Chem. B* 5 (2017) 7831–7838.
- [45] S.W. Shi, Y.H. Li, Q.L. Zhang, S.P. Yang, J.G. Liu, *J. Mater. Chem. B* 7 (2019) 1867–1874.
- [46] Q.J. He, D.O. Kiesewetter, Y. Qu, X. Fu, J. Fan, P. Huang, Y.J. Liu, G.Z. Zhu, Y. Liu, Z.Y. Qian, X.Y. Chen, *Adv. Mater.* 27 (2015) 6741–6746.
- [47] S.M. Feng, D.D. Liu, W.Y. Feng, G.Q. Feng, *Anal. Chem.* 89 (2017) 3754–3760.
- [48] D. Wu, X.H. Duan, Q.Q. Guan, J. Liu, X. Yang, F. Zhang, P. Huang, J. Shen, X. T. Shuai, Z. Cao, *Adv. Funct. Mater.* 29 (2019) 1900095.